



Recent progress in structure and dynamics of dual-membrane-spanning bacterial nanomachines

Vicki Gold¹ and Mikhail Kudryashev^{2,3}

Advances in hard-ware and soft-ware for electron cryo-microscopy and tomography have provided unprecedented structural insights into large protein complexes in bacterial membranes. Tomographic volumes of native complexes *in situ*, combined with other structural and functional data, reveal functionally important conformational changes. Here, we review recent progress in elucidating the structure and mechanism of dual-membrane-spanning nanomachines involved in bacterial motility, adhesion, pathogenesis and biofilm formation, including the type IV pilus assembly machinery and the type III and VI secretions systems. We highlight how these new structural data shed light on the assembly and action of such machines and discuss future directions for more detailed mechanistic understanding of these massive, fascinating complexes.

Addresses

¹ Department of Structural Biology, Max Planck Institute of Biophysics, Max-von-Laue Str. 3, 60438 Frankfurt am Main, Germany

² Max Planck Institute of Biophysics, Max-von-Laue Str. 3, 60438 Frankfurt am Main, Germany

³ Buchmann Institute for Molecular Life Sciences, Goethe University of Frankfurt, Max-von-Laue Str. 17, 60438 Frankfurt am Main, Germany

Corresponding authors: Gold, Vicki (vicki.gold@biophys.mpg.de) and Kudryashev, Mikhail (misha.kudryashev@biophys.mpg.de)

Current Opinion in Structural Biology 2016, 39:1–7

This review comes from a themed issue on **Membranes**

Edited by **Jacqui Gulbis** and **Gabriel Waksman**

For a complete overview see the [Issue](#) and the [Editorial](#)

Available online 17th March 2016

<http://dx.doi.org/10.1016/j.sbi.2016.03.001>

0959-440X/© 2016 The Authors. Published by Elsevier Ltd. This is an open access article under the CC BY-NC-ND license (<http://creativecommons.org/licenses/by-nc-nd/4.0/>).

Introduction

A distinctive feature of all Gram-negative bacteria is that they have two membranes — a relatively porous outer membrane and an impermeable cytoplasmic membrane. Sandwiched between them is the densely crowded periplasm and shape-determining peptidoglycan layer. Bacteria have evolved highly specialized protein machineries that span both membranes, enabling complex functions, such as cell movement [1] and molecular targeting, including protein secretion and DNA uptake [2]. Pathogenic and symbiotic Gram-negative bacteria interact with other cells by secreting effector proteins across both bacterial membranes, into the extracellular matrix or

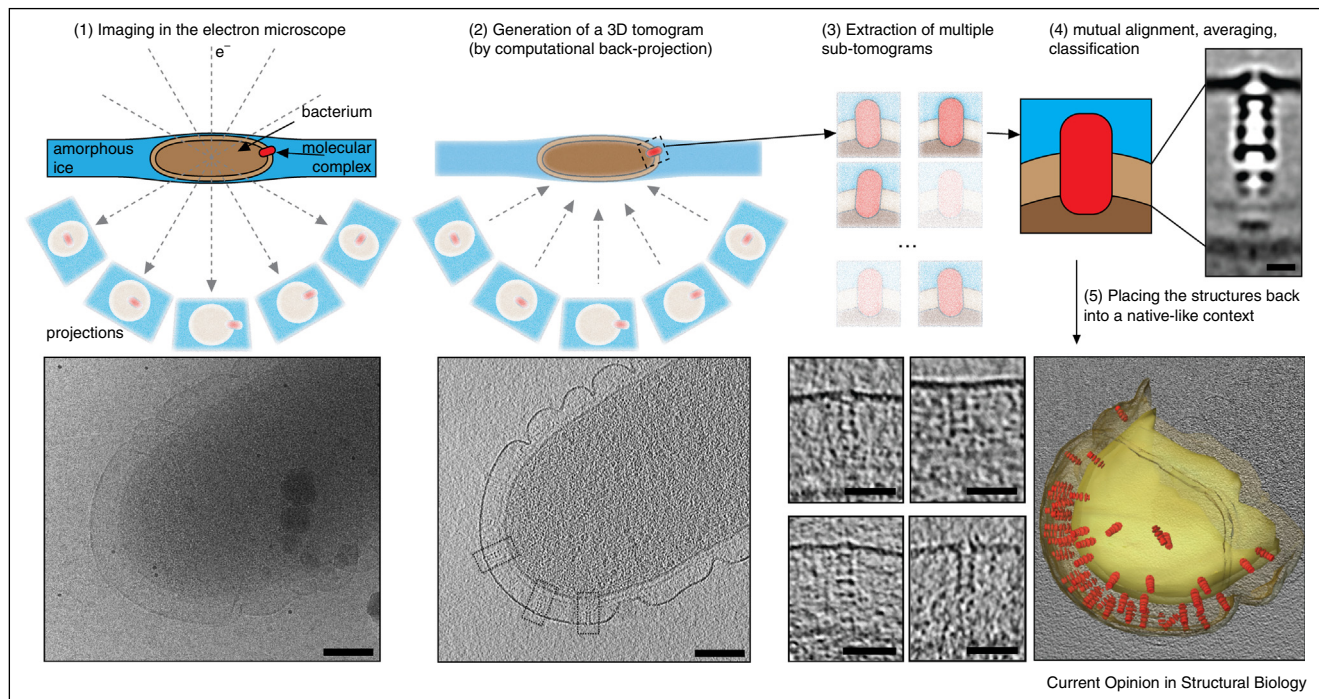
directly into host cells [3]. The mechanistic complexity of these nanomachines is achieved by assembling multiple copies of more than 20 different proteins, including both soluble and membrane-anchored subunits as structural and regulatory elements [4]. Understanding their molecular mechanism requires a combination of structural biology with genetic tools and functional studies. Some of the most pertinent questions are: how do dual-membrane spanning nanomachines assemble in order to perform their biological function? What is their mode of action? How is communication between different subunits regulated and controlled?

Recent advances in single-particle electron cryo-microscopy (cryo-EM) have made it possible to determine structures of isolated proteins or complexes at near-atomic resolution [5]. However, a major technical challenge associated with studies of large multi-component membrane protein complexes is the difficulty of purifying them in an intact state. Electron cryo-tomography (cryo-ET) enables large protein complexes inside cells to be observed in 3D at a resolution of several nanometers, by tilting a sample through a series of increments [6,7]. The resolution may be further improved by sub-tomogram averaging (StA), whereby multiple copies of the same protein or protein complex are mutually aligned and added together (Figure 1). This can yield sub-nanometer resolution, sufficient to distinguish protein domains [8] or even secondary structure [9*]. Integration of higher-resolution information obtained by single particle cryo-EM or X-ray crystallography into the StA density maps provides detailed mechanistic understanding at the level of the entire complex [8,10,11]. In addition, trapping of specific physiological states or computational classification of different protein subsets can yield intermediates of assembly and function. Here, we review recent exciting insights into structure and dynamics of the type IV pili (T4P) assembly machinery, and of the type III and VI secretion systems (T3SS/T6SS) in bacteria [3], obtained by cryo-EM and cryo-ET.

Requirements for *in situ* structural analysis

Several technical aspects need to be considered for structural determination of bacterial membrane protein complexes *in situ*. Firstly, sample thickness places a strict limit on the quality of tomographic volumes. In practice this means a maximum thickness of 400–500 nm. It is possible to reduce cell thickness by optimizing culture conditions [12], genetically engineering thin cells or small minicells [13], or by physical sectioning of the frozen bacteria with a

Figure 1



Workflow for structure determination of protein complexes *in situ* by cryo-ET and StA. **(1)** Top panel: bacterial cells embedded in a layer of amorphous ice are imaged in the electron microscope. Incremental tilts of the sample yield a series of projections from different viewing angles. The mutual orientations of the bacterium (brown) and the macromolecular complex of interest (red) vary depending on the projection angle. Bottom panel: a 0° tilt projection image of a *T. thermophilus* cell pole. Scale bar, 100 nm. **(2)** Top panel: a three-dimensional tomogram is reconstructed from the two-dimensional image series by computational back-projection. Multiple sub-tomograms containing the molecule of interest are identified and computationally cropped out of the tomogram for StA. Bottom panel: a slice through a reconstructed tomogram of the cell shown in step (1). Closed T4P (pilus retracted) complexes seen in the periplasm are boxed. Scale bar, 100 nm. **(3)** Top panel: noisy sub-tomograms with anisotropic resolution are extracted from the full volume. Bottom panel: a series of extracted sub-tomograms containing the closed state of the T4P machinery. Scale bar, 50 nm. **(4)** Left panel: particles are aligned, averaged, and classified to recover the structure of the initial object. Right panel: sub-tomogram average of the T4P machinery in the closed state [41]. Scale bar, 10 nm. **(5)** Structures are placed back into three-dimensional space in order to visualize their distribution in the native-like context. The closed state of the T4P machinery (red) is shown at the cell pole, localized between the inner membrane (yellow) and outer membrane (transparent brown).

diamond knife [14] or a focused ion beam [15]. Secondly, cryo-EM has benefitted greatly from direct electron detector cameras [16] and phase plates [17], generating high quality data in a high-throughput and automated manner. Thirdly, an inherent problem with cryo-ET is the ‘missing wedge’ of information, resulting in resolution anisotropy in the direction of the electron beam [18]. The missing wedge results from the current physical inability to rotate the sample in the microscope by a full 180°. Effects of uneven sampling are alleviated or eliminated by averaging particles in different orientations by StA [19]. Fourthly, large membrane protein complexes are often flexible, resulting in variable low-resolution maps. Conformational flexibility may be reduced biochemically, for example by cross-linking [20], or genetically, by introduction of stabilizing mutations or truncations, which carry the disadvantage of compromising the native state of the complex. Alternatively, computational methods of classification can be used to quantify and account for flexibility [21]. Finally, a prerequisite for both classification and high resolution is

the collection of very large particles data sets. Parallel and GPU-enhanced software, and thorough image analysis helps to obtain unbiased structures and structural intermediates [21–24].

Bacterial type IV pilus assembly machinery

The type IV pilus is a surface-exposed filamentous protein polymer that is several μm long, anchored to cells of evolutionarily divergent Gram-negative and Gram-positive bacteria [25]. In Gram-negative bacteria, the assembly machinery forms a multimeric dual-membrane-spanning protein supercomplex [26]. T4P play an important role in cell motility, enabling cells to adhere to and move along surfaces, form colonies and biofilms [1], and can even act as nanowires carrying electrical current [27]. Pathogenic proteobacteria, such as *Pseudomonas aeruginosa* and *Neisseria meningitidis*, use T4P to mediate adhesion to host cells prior to infection [28,29]. The machinery that assembles T4P is also implicated in DNA uptake, which is critical for lateral gene transfer and adaptive evolution [2]. The T4P is

related to both the archaeal equivalent (the archaellum) [30], and the bacterial type II secretion system (T2SS) [31], which in some bacteria secretes proteins and toxins into the extracellular environment.

The composition of pili varies between species, but they are predominantly formed of an oligomer of the major pilin protein (PilA in *Pseudomonas* and *Thermus*, PilE in *Neisseria*) plus a few copies of different minor pilins [32]. X-ray structures of several major pilins have been reported [32], demonstrating a conserved fold and a characteristic 'lollipop' shape. A pseudo-atomic model of a filamentous pilus from *Neisseria gonorrhoeae* was built by docking X-ray structures of pilin subunits into a cryo-EM map of isolated pili, which were ~6 nm wide with a narrow central channel of ~1 nm [33]. Studies of multiple species, including *N. meningitidis* [34] and *Thermus thermophilus* [2], have shown that pre-pilins mature by the action of a peptidase (PilD), then assemble at the inner membrane by a AAA-ATPase (PilF) with the help of additional proteins, including PilM, PilN and PilO. The pilus is directed across the outer membrane through the pore of a large multimeric ~1 MDa secretin protein (PilQ), which in *Thermus* is formed by a membrane-embedded cone-like structure with a series of 6 stacked rings in the periplasm [35]. Bacterial T4P are unique in that they can be rapidly retracted through the action of a cytoplasmic AAA-ATPase (PilT). Retraction results in forces of 100 pN per single motor [36], making the T4P machinery the most powerful molecular machine studied to date. It is this combined action of assembly, surface adherence and then retraction that enables cells to move in a jerky fashion, referred to as 'twitching' [37,38].

Whilst there have been numerous structural studies of the bacterial flagellar motor and associated motility [39,40], very little was known about the *in situ* structure and supramolecular assembly of a twitching machinery until recently. Using cryo-ET of whole bacterial cells, Gold and colleagues investigated the intact T4P machinery of *T. thermophilus in situ* [41**] (Figures 1 and 2a). In order to render the cells thin enough for reliable particle identification and StA, the sample was treated with EDTA, which revealed large transmembrane T4P complexes bridging both membranes at the cell poles [41**]. By analysis of different conformational states, the structure of the machinery was determined in the closed (pilus retracted) and open (pilus assembled) conformation. Evidently, the PilQ secretin is extremely dynamic and undergoes a large 30 Å shift of periplasmic N-terminal domains and widening of the central pore on channel opening to make way for the assembled pilus (Figure 2a). The diameter of the pilus was narrower than previously reported [33] suggesting that different forms may exist. Additional protein density was visible in the cytoplasm in the open state of the complex only. It follows that the

ATPases (PilF/PilT) required for pilus assembly and retraction may contribute to this density.

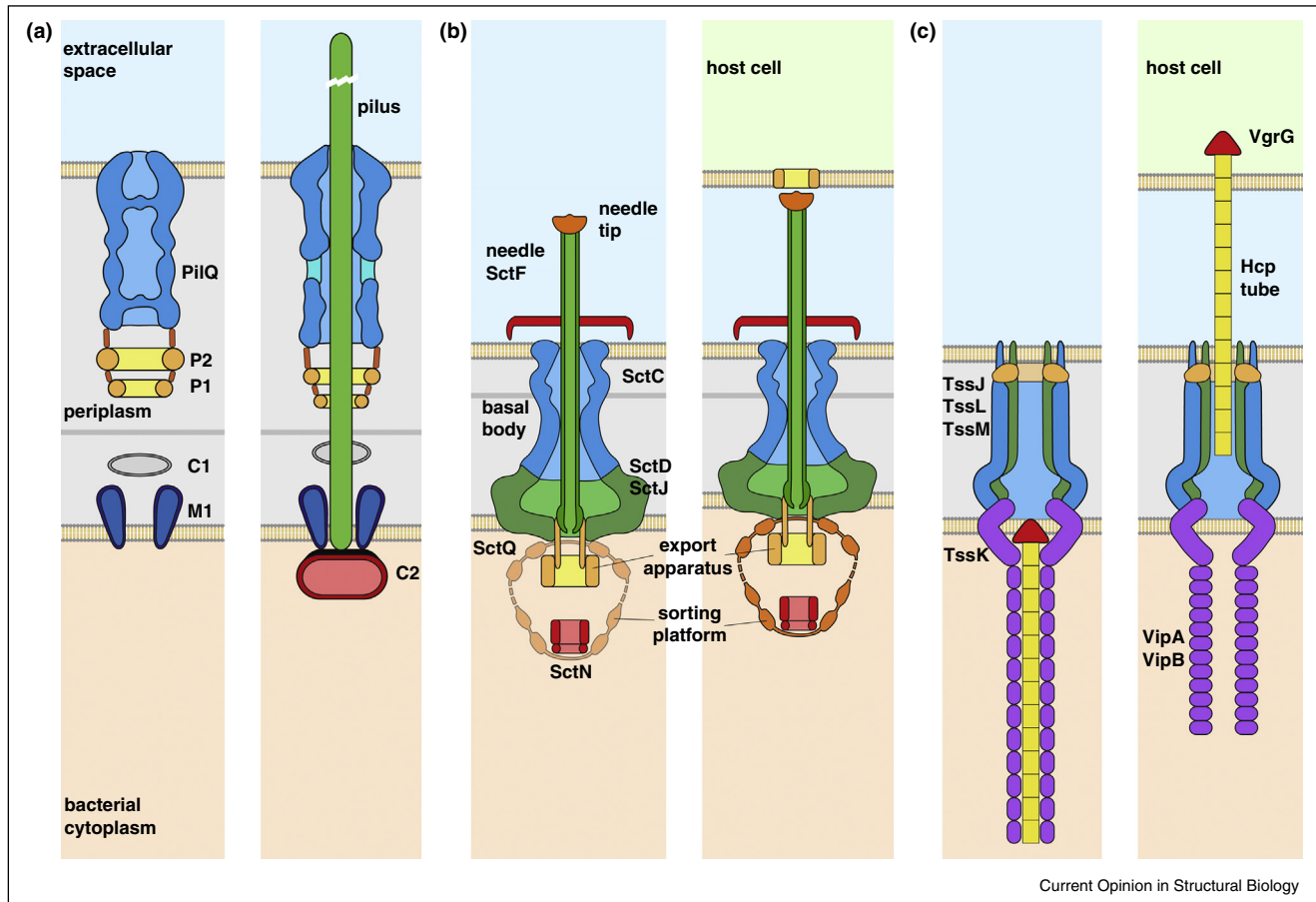
A prerequisite for complete understanding of the assembly and dynamics of the various protein components in the T4P machinery is the assignment of specific densities within the electron density maps, and determination of complete high-resolution structural information. X-ray structures are available for a few proteins, their homologues or small fragments [42–49]. Identification of these proteins within the supercomplex will require a combination of genetic manipulation and/or protein labeling [50,51] with functional studies and further structural determination. Fitting high-resolution structures into their corresponding density in cryo-ET maps will provide important future insights into the composition and functionality of these highly dynamic and versatile molecular machines.

Bacterial type III secretion systems

The type III secretion system (T3SS or injectisome) is a machinery that is commonly used to deliver bacterial effectors from the cytoplasm directly into the cytosol of a target cell [52,53] in an ATP-dependent manner. The T3SS is composed of a basal body spanning the bacterial periplasm (StcC, SctD and SctJ according to the unified nomenclature [54]), a hollow needle extending into the extracellular space (SctF) and a cytoplasmic part containing the T3S export apparatus (SctV, SctR, SctS and SctT), a sorting platform (SctQ, SctL and SctK) [55] and an ATPase SctN (Figure 2b). The cytoplasmic part of the T3SS is evolutionarily related to its counterpart from the bacterial flagellar motor, responsible for assembly and secretion [56]. The ATPase SctN is structurally similar to both F-type and V-type ATPases [57] and is thought to be responsible for detachment of chaperones and unfolding the exported substrate [58]. Intact injectisomes were recently observed by cryo-ET inside native *Yersinia enterocolitica* [59], *Salmonella enterica* [60] and *Shigella flexneri* [59,61**]. In all cases the best resolution was obtained with bacterial minicells, which were shown to have active T3SS in *Salmonella* [62]. The periplasmic component of *Yersinia* injectisomes varied in length by ~20%, suggesting that its flexibility may be important for the secretion process. The 27 Å resolution structure of the *S. flexneri* injectisome by Hu and colleagues [61**] allowed unambiguous localization of the basal body. The proteins of the sorting platform that were poorly resolved in previous structures were clearly visible: hexameric SctN is axially aligned to the C-ring, composed of SctQ, by six radial spokes of SctL [61**]. Such positioning allows transport of partially unfolded proteins from SctN to the pore in the export apparatus protein SctV [61**] and further through the needle to the host cell.

Recent fluorescent studies in *Yersinia* demonstrating turnover of SctQ suggest that the T3SS is a highly dynamic

Figure 2



Cross section models of dual-membrane-spanning bacterial protein machines in the inactive and active state. **(a)** The T4P machinery, based on the *in situ* structure from *T. thermophilus*. The PilQ secretin (blue) is shown embedded in the outer membrane and extends to the centre of the periplasm and peptidoglycan layer (grey line). Two gates enclose a periplasmic vestibule, which open on pilus assembly (green). Additional protein densities, of which the identities are currently unclear, are seen to associate with PilQ to build the entire machinery (C1, P1, P2) as previously assigned [41]. Protein densities P1 and P2 (yellow) form rings, which are likely attached to PilQ by linker domains (orange) that are not resolved in the sub-tomogram average. Protein C1 (grey) may be comprised of the soluble part of inner membrane anchored proteins M1 (dark blue), such as PilC, PilN or PilO, which are thought to form part of the inner membrane assembly platform for pilus biogenesis [2,44,45]. A large cytoplasmic protein density C2 (red) is visible in the open state only. Candidate proteins include PilM and the ATPases PilF and PilT1/2. **(b)** Model of the T3SS based on the *in situ* structure of the complex from *Chlamydia trachomatis*: the basal body consisting of SctC (blue), SctD and SctJ (green) contracts during secretion. The needle, composed of SctF (green) extends into the extracellular space, reaching the host cell membrane with the needle tip (top, orange). The extracellular plate (red) is *Chlamydia* – specific and not observed in other studies of T3SS; peptidoglycan layer (grey line) is observed in most of T3SS-containing bacteria, but not in *C. trachomatis*. Upon activation, the cytoplasmic density of the sorting platform, which aligns the SctN ATPase and the export apparatus, becomes more ordered. **(c)** Model for T6SS secretion. Left: T6SS in a resting state contains a periplasm-spanning part comprised of TssJ, TssL and TssM [76], an inner tube made of the Hcp protein containing effectors (yellow) and an extended sheath made of VipA/VipB (purple). Prompted by an as yet unknown trigger, the sheath contracts to release the Hcp tube into the host cell. The following steps are disassembly of the contracted sheath by a ClpV ATPase and re-building of a new T6SS.

machine [63]. This turnover rate was faster for secreting injectisomes and required the ATPase SctN for stabilization in the non-secreting state [63]. Finally, upon activation of secretion, assembly of new injectisomes occurs close to the existing ones [64]. Nans and colleagues visualized large conformational changes associated with activation of injectisomes of *Chlamydia trachomatis* during host membrane contact with the cultured human cells [65•]. The periplasmic basal body contracted by 4–5 nm leading to an extension of the needle outside the bacteria

reaching the host-cell membrane (Figure 2b). In the secreting state the sorting platform was significantly better defined on the cytoplasmic side, suggesting that ordering of the sorting platform is related to the ‘pump-like’ contraction of the basal body.

A combination of higher-resolution structures in both secreting and non-secreting states with computational analysis [59,66,67] and genetic manipulation will advance mechanistic understanding of injectisomes and

how secretion is regulated. However, there is as yet no obvious model system. The injectisome from *S. flexneri* has already been visualized in direct contact with a red blood cell [61**] and its proteins are easy to modify, providing an opportunity to genetically dissect the machinery and mechanism. Data collection for structural analysis will be challenging due to the limited number of injectisomes per *S. flexneri* minicell. *Chlamydia* on the other hand, whilst more difficult to modify genetically, are naturally small, contain numerous injectisomes and may be imaged inside thin human cells [65**,68]. In the future it may be possible to analyze structural changes associated to T3S *in situ* based on a combination of model systems.

Bacterial type VI secretion systems

Pathogenic bacteria, such as *Vibrio cholerae* and *P. aeruginosa*, use the T6SS to kill both eukaryotic and prokaryotic cells [69]. 25% of all Gram-negative bacteria have at least one T6SS gene cluster [70]. Based on remote sequence similarity to the tailed bacteriophage T4 [71], the T6SS is described as an inverted phage located inside the bacterial cytoplasm (Figure 2c). It contains a baseplate spanning the two bacterial membranes, followed by a long inner tube covered by an outer sheath. Analogous to phages, the energy for a single secretion ‘shot’ has been suggested to be stored in the conformational energy of the sheath. An unknown trigger causes the energy to be converted into mechanical motion [71]. Basler and colleagues revealed dynamics of the *V. cholerae* T6SS by combining fluorescence microscopy and cryo-ET. The sheath polymerizes at the cytoplasmic membrane, forming $\sim 1 \mu\text{m}$ filled tubes. Upon contraction, the length of the sheath decreases roughly twofold, the radius increases and the tube appears empty, suggesting that the contents of the inner tube are released to the outside of the cell [72].

Structures of entire T6SS *in situ* are not yet available, due to the large thickness of cells that typically contain this system. However, important structural insights have been gained by single-particle cryo-EM. Atomic structures of native contracted sheaths purified from *V. cholerae* [73*] and *Francisella tularensis* [74*] demonstrated a high degree of similarity between the inner domains of the T6SS and bacteriophage sheaths, while the outer domains were more divergent. The interaction between sheath subunits is organized in a 6-start helix, by a network of tightly interacting beta strands; in both cases this network was shown to be critical for assembly and contraction of the T6SS. Using cryo-EM, Ge *et al.* [75] revealed the contraction mechanism of R-type pyocins, which share high similarity to the inner domains of the both T6SS and phage sheaths; this data may be used to model the conformational changes occurring during sheath contraction. Remaining questions include a mechanistic understanding of effector packing into the T6SS, details of selective recycling of contracted sheaths and conformational changes occurring in the

periplasmic baseplate related to effector secretion. Finally, the membrane-spanning core complex composed of TssJ, TssL and TssM from pathogenic *E. coli* revealed by negative stain EM was shown to be five-fold symmetric [76], raising the question of how it can be attached to a sheath with C6 symmetry. *In situ* structural approaches may shed light on these questions, however, again this depends on a good model system. The classical model systems *V. cholerae* and *P. aeruginosa* are thicker than 500–700 nm, limiting high-resolution cryo-ET.

In a recent StA structure of the *Myxococcus xanthus* type IVa pilus machinery [77], the locations of individual proteins were identified in the complex, leading to a working model for mechanism of action.

Future directions

In situ structural analysis is now one of the key tools to study the structure and function of large membrane complexes in a close-to-native state. Combining this approach with high-resolution structures that result from the wider use of advanced instrumentation and genetic and biochemical manipulations such as gene knock-outs [5] and electron-dense labeling [50,51] will aid in the identification of individual components in density maps. In particular, structural analysis in defined functional states will help to understand the conformational changes associated with function. Supportive biochemical functional studies, fluorescence imaging and molecular simulations should then enable a complete mechanistic understanding of action. We describe how observation of large multimeric complexes *in situ* is extremely informative and may promote application of similar methodology to study other dynamic membrane protein systems.

Note added in proof

In a recent StA structure of the *Myxococcus xanthus* type IVa pilus machinery [77], the locations of individual proteins were identified in the complex, leading to a working model for mechanism of action.

Conflict of interest statement

Nothing declared.

Acknowledgements

We thank Werner Kühlbrandt for support and helpful discussions, and Paolo Lastrico for help with graphics. We gratefully acknowledge Beate Averhoff, Marek Basler, Andrea Nans and Bertram Daum for their comments on this manuscript. This work was supported by the Max Planck Society and a Sofja Kovalevskaja Award from the Humboldt Foundation (to MK).

References and recommended reading

Papers of particular interest, published within the period of review, have been highlighted as:

- of special interest
- of outstanding interest

1. Maier B, Wong GC: **How bacteria use type IV pili machinery on surfaces.** *Trends Microbiol* 2015, **23**:775-788.

2. Averhoff B: **Shuffling genes around in hot environments: the unique DNA transporter of *Thermus thermophilus***. *FEMS Microbiol Rev* 2009, **33**:611-626.
3. Costa TR, Felisberto-Rodrigues C, Meir A, Prevost MS, Redzej A, Trokter M, Waksman G: **Secretion systems in Gram-negative bacteria: structural and mechanistic insights**. *Nat Rev Microbiol* 2015, **13**:343-359.
4. Diepold A, Wagner S: **Assembly of the bacterial type III secretion machinery**. *FEMS Microbiol Rev* 2014, **38**:802-822.
5. Zhao X, Zhang K, Boquoi T, Hu B, Motaleb MA, Miller KA, James ME, Charon NW, Manson MD, Norris SJ *et al.*: **Cryo-electron tomography reveals the sequential assembly of bacterial flagella in *Borrelia burgdorferi***. *Proc Natl Acad Sci U S A* 2013, **110**:14390-14395.
6. Lucic V, Rigort A, Baumeister W: **Cryo-electron tomography: the challenge of doing structural biology *in situ***. *J Cell Biol* 2013, **202**:407-419.
7. Davies KM, Daum B, Gold VA, Mühleip AW, Brandt T, Blum TB, Mills DJ, Kühlbrandt W: **Visualization of ATP synthase dimers in mitochondria by electron cryo-tomography**. *J Vis Exp: JoVE* 2014:51228.
8. von Appen A, Kosinski J, Sparks L, Ori A, DiGiulio AL, Vollmer B, Mackmull MT, Banterle N, Parca L, Kasttris P *et al.*: ***In situ* structural analysis of the human nuclear pore complex**. *Nature* 2015, **526**:140-143.
9. Schur FK, Hagen WJ, Rumlova M, Ruml T, Muller B, Krausslich HG, Briggs JA: **Structure of the immature HIV-1 capsid in intact virus particles at 8.8 Å resolution**. *Nature* 2015, **517**:505-508.
- The authors performed cryo-ET and StA on native HIV-1 virions and obtained a reconstruction of the Gag capsid lattice at sub-nanometer resolution. This structure allowed unambiguous positioning of all helices and generation of a model that revealed structural interactions mediating HIV-1 assembly.
10. Dodonova SO, Diestelkoetter-Bachert P, von Appen A, Hagen WJ, Beck R, Beck M, Wieland F, Briggs JA: **VESICULAR TRANSPORT. A structure of the COPI coat and the role of coat proteins in membrane vesicle assembly**. *Science* 2015, **349**:195-198.
11. Bharat TA, Murshudov GN, Sachse C, Lowe J: **Structures of actin-like ParM filaments show architecture of plasmid-segregating spindles**. *Nature* 2015, **523**:106-110.
12. Ortiz JO, Brandt F, Matias VR, Sennels L, Rappsilber J, Scheres SH, Eibauer M, Hartl FU, Baumeister W: **Structure of hibernating ribosomes studied by cryo-electron tomography *in vitro* and *in situ***. *J Cell Biol* 2010, **190**:613-621.
13. Liu J, Chen CY, Shiomi D, Niki H, Margolin W: **Visualization of bacteriophage P1 infection by cryo-electron tomography of tiny *Escherichia coli***. *Virology* 2011, **417**:304-311.
14. Zuber B, Chami M, Houssin C, Dubochet J, Griffiths G, Daffe M: **Direct visualization of the outer membrane of mycobacteria and corynebacteria in their native state**. *J Bacteriol* 2008, **190**:5672-5680.
15. Mahamid J, Schampers R, Persoon H, Hyman AA, Baumeister W, Plietzko JM: **A focused ion beam milling and lift-out approach for site-specific preparation of frozen-hydrated lamellas from multicellular organisms**. *J Struct Biol* 2015, **192**:262-269.
16. Kühlbrandt W: **Biochemistry. The resolution revolution**. *Science* 2014, **343**:1443-1444.
17. Asano S, Fukuda Y, Beck F, Aufderheide A, Förster F, Danev R, Baumeister W: **Proteasomes. A molecular census of 26S proteasomes in intact neurons**. *Science* 2015, **347**:439-442.
18. Palmer CM, Lowe J: **A cylindrical specimen holder for electron cryo-tomography**. *Ultramicroscopy* 2014, **137**:20-29.
19. Briggs JA: **Structural biology *in situ* — the potential of subtomogram averaging**. *Curr Opin Struct Biol* 2013, **23**:261-267.
20. Kastner B, Fischer N, Golas MM, Sander B, Dube P, Boehringer D, Hartmuth K, Deckert J, Hauer F, Wolf E *et al.*: **GraFix: sample preparation for single-particle electron cryomicroscopy**. *Nat Methods* 2008, **5**:53-55.
21. Scheres SH: **RELION: implementation of a Bayesian approach to cryo-EM structure determination**. *J Struct Biol* 2012, **180**:519-530.
22. Castano-Diez D, Kudryashev M, Arheit M, Stahlberg H: **Dynamo: a flexible, user-friendly development tool for subtomogram averaging of cryo-EM data in high-performance computing environments**. *J Struct Biol* 2012, **178**:139-151.
23. Pymol. The PyMOL Molecular Graphics System, Version 1.7.4 Schrödinger, LLC.
24. Nicastro D, Schwartz C, Pierson J, Gaudette R, Porter ME, McIntosh JR: **The molecular architecture of axonemes revealed by cryo-electron tomography**. *Science* 2006, **313**:944-948.
25. Pelicic V: **Type IV pili: *e pluribus unum*?** *Mol Microbiol* 2008, **68**:827-837.
26. Craig L, Li J: **Type IV pili: paradoxes in form and function**. *Curr Opin Struct Biol* 2008, **18**:267-277.
27. Malvankar NS, Lovley DR: **Microbial nanowires: a new paradigm for biological electron transfer and bioelectronics**. *Chem Sus Chem* 2012, **5**:1039-1046.
28. Plant LJ, Jonsson AB: **Type IV pili of *Neisseria gonorrhoeae* influence the activation of human CD4+ T cells**. *Infect Immun* 2006, **74**:442-448.
29. O'Toole GA, Kolter R: **Flagellar and twitching motility are necessary for *Pseudomonas aeruginosa* biofilm development**. *Mol Microbiol* 1998, **30**:295-304.
30. Albers SV, Jarrell KF: **The archaeellum: how Archaea swim**. *Front Microbiol* 2015, **6**:23.
31. Ayers M, Howell PL, Burrows LL: **Architecture of the type II secretion and type IV pilus machineries**. *Future Microbiol* 2010, **5**:1203-1218.
32. Giltner CL, Nguyen Y, Burrows LL: **Type IV pilin proteins: versatile molecular modules**. *Microbiol Mol Biol Rev* 2012, **76**:740-772.
33. Craig L, Volkman N, Arvai AS, Pique ME, Yeager M, Egelman EH, Tainer JA: **Type IV pilus structure by cryo-electron microscopy and crystallography: implications for pilus assembly and functions**. *Mol Cell* 2006, **23**:651-662.
34. Carbonnelle E, Helaine S, Nassif X, Pelicic V: **A systematic genetic analysis in *Neisseria meningitidis* defines the Pil proteins required for assembly, functionality, stabilization and export of type IV pili**. *Mol Microbiol* 2006, **61**:1510-1522.
35. Burkhardt J, Vonck J, Averhoff B: **Structure and function of PilQ, a secretin of the DNA transporter from the thermophilic bacterium *Thermus thermophilus* HB27**. *J Biol Chem* 2011, **286**:9977-9984.
36. Maier B, Potter L, So M, Long CD, Seifert HS, Sheetz MP: **Single pilus motor forces exceed 100 pN**. *Proc Natl Acad Sci U S A* 2002, **99**:16012-16017.
37. Mattick JS: **Type IV pili and twitching motility**. *Annu Rev Microbiol* 2002, **56**:289-314.
38. Burrows LL: ***Pseudomonas aeruginosa* twitching motility: type IV pili in action**. *Annu Rev Microbiol* 2012, **66**:493-520.
39. Jarrell KF, McBride MJ: **The surprisingly diverse ways that prokaryotes move**. *Nat Rev Microbiol* 2008, **6**:466-476.
40. Chen S, Beeby M, Murphy GE, Leadbetter JR, Hendrixson DR, Briegel A, Li Z, Shi J, Tocheva EI, Muller A *et al.*: **Structural diversity of bacterial flagellar motors**. *EMBO J* 2011, **30**:2972-2981.
41. Gold VA, Salzer R, Averhoff B, Kühlbrandt W: **Structure of a type IV pilus machinery in the open and closed state**. *eLife* 2015, **4**:e07380.
- In this study the authors determine the first *in situ* structure of a T4P assembly machinery by cryo-ET and StA. Structures were determined for the closed (pilus retracted) and open (pilus assembled) state, which revealed a large conformational change associated with channel opening.
42. Trindade MB, Job V, Contreras-Martel C, Pelicic V, Dessen A: **Structure of a widely conserved type IV pilus biogenesis factor**

- that affects the stability of secretin multimers. *J Mol Biol* 2008, **378**:1031-1039.
43. Sampaleanu LM, Bonanno JB, Ayers M, Koo J, Tammam S, Burley SK, Almo SC, Burrows LL, Howell PL: **Periplasmic domains of *Pseudomonas aeruginosa* PilN and PilO form a stable heterodimeric complex.** *J Mol Biol* 2009, **394**:143-159.
 44. Karuppiah V, Derrick JP: **Structure of the PilM-PilN inner membrane type IV pilus biogenesis complex from *Thermus thermophilus*.** *J Biol Chem* 2011, **286**:24434-24442.
 45. Karuppiah V, Collins RF, Thistlethwaite A, Gao Y, Derrick JP: **Structure and assembly of an inner membrane platform for initiation of type IV pilus biogenesis.** *Proc Natl Acad Sci U S A* 2013, **110**:E4638-E4647.
 46. Karuppiah V, Hassan D, Saleem M, Derrick JP: **Structure and oligomerization of the PilC type IV pilus biogenesis protein from *Thermus thermophilus*.** *Proteins* 2010, **78**:2049-2050.
 47. Kim K, Oh J, Han D, Kim EE, Lee B, Kim Y: **Crystal structure of PilF: functional implication in the type 4 pilus biogenesis in *Pseudomonas aeruginosa*.** *Biochem Biophys Res Commun* 2006, **340**:1028-1038.
 48. Koo J, Tammam S, Ku SY, Sampaleanu LM, Burrows LL, Howell PL: **PilF is an outer membrane lipoprotein required for multimerization and localization of the *Pseudomonas aeruginosa* Type IV pilus secretin.** *J Bacteriol* 2008, **190**:6961-6969.
 49. Satyshur KA, Worzalla GA, Meyer LS, Heiniger EK, Aukema KG, Mistic AM, Forest KT: **Crystal structures of the pilus retraction motor PilT suggest large domain movements and subunit cooperation drive motility.** *Structure* 2007, **15**:363-376.
 50. Gold VA, Ieva R, Walter A, Pfanner N, van der Laan M, Kühlbrandt W: **Visualizing active membrane protein complexes by electron cryotomography.** *Nat Commun* 2014, **5**:4129.
 51. Diestra E, Fontana J, Guichard P, Marco S, Risco C: **Visualization of proteins in intact cells with a clonable tag for electron microscopy.** *J Struct Biol* 2009, **165**:157-168.
 52. Cornelis GR: **The type III secretion injectisome.** *Nat Rev Microbiol* 2006, **4**:811-825.
 53. Galan JE, Wolf-Watz H: **Protein delivery into eukaryotic cells by type III secretion machines.** *Nature* 2006, **444**:567-573.
 54. Hueck CJ: **Type III protein secretion systems in bacterial pathogens of animals and plants.** *Microbiol Mol Biol Rev* 1998, **62**:379-433.
 55. Lara-Tejero M, Kato J, Wagner S, Liu X, Galán JE: **A sorting platform determines the order of protein secretion in bacterial type III systems.** *Science* 2011, **331**:1188-1191.
 56. Diepold A, Armitage JP: **Type III secretion systems: the bacterial flagellum and the injectisome.** *Philos Trans R Soc Lond B Biol Sci* 2015:370.
 57. Ibuki T, Imada K, Minamino T, Kato T, Miyata T, Namba K: **Common architecture of the flagellar type III protein export apparatus and F- and V-type ATPases.** *Nat Struct Mol Biol* 2011, **18**:277-282.
 58. Akeda Y, Galan JE: **Chaperone release and unfolding of substrates in type III secretion.** *Nature* 2005, **437**:911-915.
 59. Kudryashev M, Stenta M, Schmelz S, Amstutz M, Wiesand U, Castano-Diez D, Degiacomi MT, Munnich S, Bleck CK, Kowal J *et al.*: **In situ structural analysis of the *Yersinia enterocolitica* injectisome.** *eLife* 2013, **2**:e00792.
 60. Kawamoto A, Morimoto YV, Miyata T, Minamino T, Hughes KT, Kato T, Namba K: **Common and distinct structural features of *Salmonella* injectisome and flagellar basal body.** *Sci Rep* 2013, **3**:3369.
 61. Hu B, Morado DR, Margolin W, Rohde JR, Arizmendi O, Picking WL, Picking WD, Liu J: **Visualization of the type III secretion sorting platform of *Shigella flexneri*.** *Proc Natl Acad Sci U S A* 2015, **112**:1047-1052.
- The authors used cryo-ET and sTA to visualize the structure of the T3SS in fine detail, allowing unambiguous positioning of the basal body in the membrane and visualization of the T3 export apparatus inside the native assembled complex.
62. Carleton HA, Lara-Tejero M, Liu X, Galan JE: **Engineering the type III secretion system in non-replicating bacterial minicells for antigen delivery.** *Nat Commun* 2013, **4**:1590.
 63. Diepold A, Kudryashev M, Delalez NJ, Berry RM, Armitage JP: **Composition, formation, and regulation of the cytosolic c-ring, a dynamic component of the type III secretion injectisome.** *PLoS Biol* 2015, **13**:e1002039.
 64. Kudryashev M, Diepold A, Amstutz M, Armitage JP, Stahlberg H, Cornelis GR: ***Yersinia enterocolitica* type III secretion injectisomes form regularly spaced clusters, which incorporate new machines upon activation.** *Mol Microbiol* 2015, **95**:875-884.
 65. Nans A, Kudryashev M, Saibil HR, Hayward RD: **Structure of a bacterial type III secretion system in contact with a host membrane in situ.** *Nat Commun* 2015, **6**:10114.
- The authors visualized structural differences between the T3SS of *Chlamydia trachomatis* in a non-active state and during secretion of effectors into the host cells by cryo-ET and sTA. The resulting pump-like contraction of the basal body by 4–5 nm was suggested to be associated with the secretion process.
66. Bergeron JR, Worrall LJ, De S, Sgourakis NG, Cheung AH, Lameignere E, Okon M, Wasney GA, Baker D, McIntosh LP *et al.*: **The modular structure of the inner-membrane ring component PrgK facilitates assembly of the type III secretion system basal body.** *Structure* 2015, **23**:161-172.
 67. Bergeron JR, Worrall LJ, Sgourakis NG, DiMaio F, Pfuetzner RA, Felise HB, Vuckovic M, Yu AC, Miller SI, Baker D *et al.*: **A refined model of the prototypical *Salmonella* SPI-1 T3SS basal body reveals the molecular basis for its assembly.** *PLoS Pathogens* 2013, **9**:e1003307.
 68. Nans A, Saibil HR, Hayward RD: **Pathogen-host reorganization during *Chlamydia* invasion revealed by cryo-electron tomography.** *Cell Microbiol* 2014, **16**:1457-1472.
 69. Basler M: **Type VI secretion system: secretion by a contractile nanomachine.** *Philos Trans R Soc Lond B Biol Sci* 2015:370.
 70. Ho BT, Dong TG, Mekalanos JJ: **A view to a kill: the bacterial type VI secretion system.** *Cell Host Microbe* 2014, **15**:9-21.
 71. Leiman PG, Basler M, Ramagopal UA, Bonanno JB, Sauder JM, Pukatzki S, Burley SK, Almo SC, Mekalanos JJ: **Type VI secretion apparatus and phage tail-associated protein complexes share a common evolutionary origin.** *Proc Natl Acad Sci U S A* 2009, **106**:4154-4159.
 72. Basler M, Pilhofer M, Henderson GP, Jensen GJ, Mekalanos JJ: **Type VI secretion requires a dynamic contractile phage tail-like structure.** *Nature* 2012, **483**:182-186.
 73. Kudryashev M, Wang RY, Brackmann M, Scherer S, Maier T, Baker D, DiMaio F, Stahlberg H, Egelman EH, Basler M: **Structure of the type VI secretion system contractile sheath.** *Cell* 2015, **160**:952-962.
- A near-atomic cryo-EM structure of the native contracted T6SS sheath isolated from *Vibrio cholerae* showed that the VipA/VipB protomer is similar to that of the T4 phage sheath. Interactions between protomers were organized by a network of beta-strands, which were shown to be required for assembly and contraction of T6SS.
74. Clemens DL, Ge P, Lee BY, Horwitz MA, Zhou ZH: **Atomic structure of T6SS reveals interlaced array essential to function.** *Cell* 2015, **160**:940-951.
- The authors confirmed the identity of the T6SS in Francisella and solved the near-atomic structure of the contracted T6SS sheath by single particle cryo-EM. The two-dimensional network of inter-protomer interactions is organized by beta strand augmentation and was found to be essential for secretion, phagosomal escape and intracellular replication of bacteria.
75. Ge P, Scholl D, Leiman PG, Yu X, Miller JF, Zhou ZH: **Atomic structures of a bactericidal contractile nanotube in its pre- and postcontraction states.** *Nat Struct Mol Biol* 2015, **22**:377-382.
 76. Durand E, Nguyen VS, Zoued A, Logger L, Pehau-Arnaudet G, Aschtgen MS, Spinelli S, Desmyter A, Bardiaux B, Dujeancourt A *et al.*: **Biogenesis and structure of a type VI secretion membrane core complex.** *Nature* 2015, **523**:555-560.
 77. Chang Y, Rettberg LA, Treuner-Lange A, Iwasa J, Søgaard-Andersen L, Jensen GJ: **Architecture of the type IVa pilus machine.** *Science* 2016, **351**.